Supplementary Information

Mechanical, compositional and morphological characterisation of the human male urethra for the development of a biomimetic tissue engineered urethral scaffold

Eoghan M. Cunnane (1,2), Niall F. Davis (2), Connor V. Cunnane (3), Katherine L. Lorentz (1), Alan J. Ryan (2), Jochen Hess (4), Justin S. Weinbaum (1,5,6), Michael T. Walsh (3), Fergal J. O'Brien (2,7,8), David A. Vorp* (1,5,9,10,11)

1 Department of Bioengineering, University of Pittsburgh, Pittsburgh, PA 15213, US.
2 Tissue Engineering Research Group, Dept. of Anatomy, Royal College of Surgeons in Ireland (RCSI), Dublin, D02 YN77, Ireland.
3 School of Engineering, Health Research Institute and the Bernal Institute, University of Limerick, Limerick, V94 T9PX, Ireland.
4 Department of Urology, University Hospital Essen, University Duisburg-Essen, 45147 Essen, Germany.
5 McGowan Institute for Regenerative Medicine, University of Pittsburgh, Pittsburgh, PA 15219, United States.
6 Department of Pathology, University of Pittsburgh, Pittsburgh, PA 15213, US.
7 Trinity Centre for Biomedical Engineering, Trinity College Dublin (TCD), Dublin, D02 R590, Ireland.
8 Advanced Materials and Bioengineering Research Centre (AMBER), RCSI and TCD, Dublin, D02 R590, Ireland.
9 Department of Surgery, University of Pittsburgh, Pittsburgh, PA 15213, US.
10 Department of Cardiothoracic Surgery, University of Pittsburgh, Pittsburgh, PA 15213, United States.
11 Department of Chemical and Petroleum Engineering, University of Pittsburgh, PA 15213, United States.

Address correspondence to:

David A. Vorp, Ph.D.
e-mail: vorp@pitt.edu

1 ARRIVE Guideline Considerations

The ARRIVE guidelines were considered when designing the animal experiment. As this is an exploratory study to determine the effect of scaffold type on cell infiltration, and future studies are planned to examine the scaffold in a more appropriate animal model, power calculations were not performed. Implants were performed in five animals to allow for sample and/or animal attrition during the experiment, while still facilitating statistical analysis of the resulting data. Prior to inclusion, animals were visibly inspected for evidence of infection (eye, urinary tract, etc.). No animals were excluded from analysis. However, one SIS implant could not be retrieved at the time of explant (n = 4 for the SIS group). Randomisation and blinding were not employed in this study as the scaffold type could be clearly distinguished at implant and explant. To remove the influence of implant location, the implant site was varied across animals for each scaffold type. All implants were performed by the same surgeon, on the same day, across a period of 5 hours. Rats were then single housed for a period of one week. The primary outcome of the study was the number of cells that infiltrate each scaffold. The secondary outcomes were the number of these cells that are CD68+ and the location of these cells within the scaffold.

2 Supplementary Figures and Tables

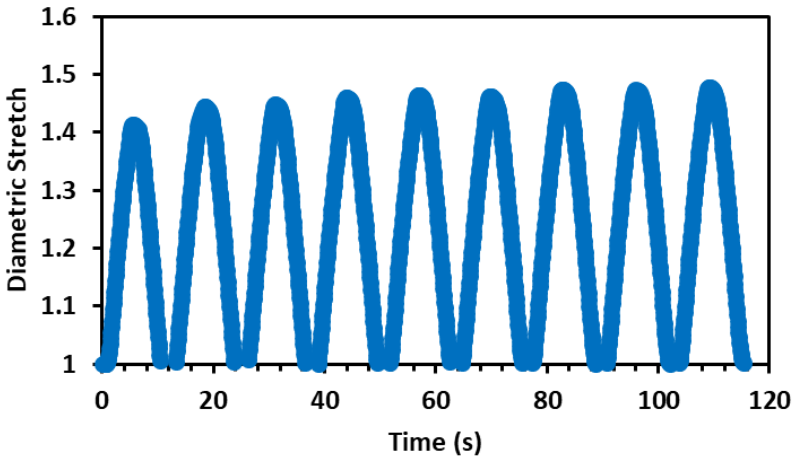

Figure S1: Strain-softening effect observed during the application of repeat intraluminal loading to 10 kPa of human urethra sample 5.

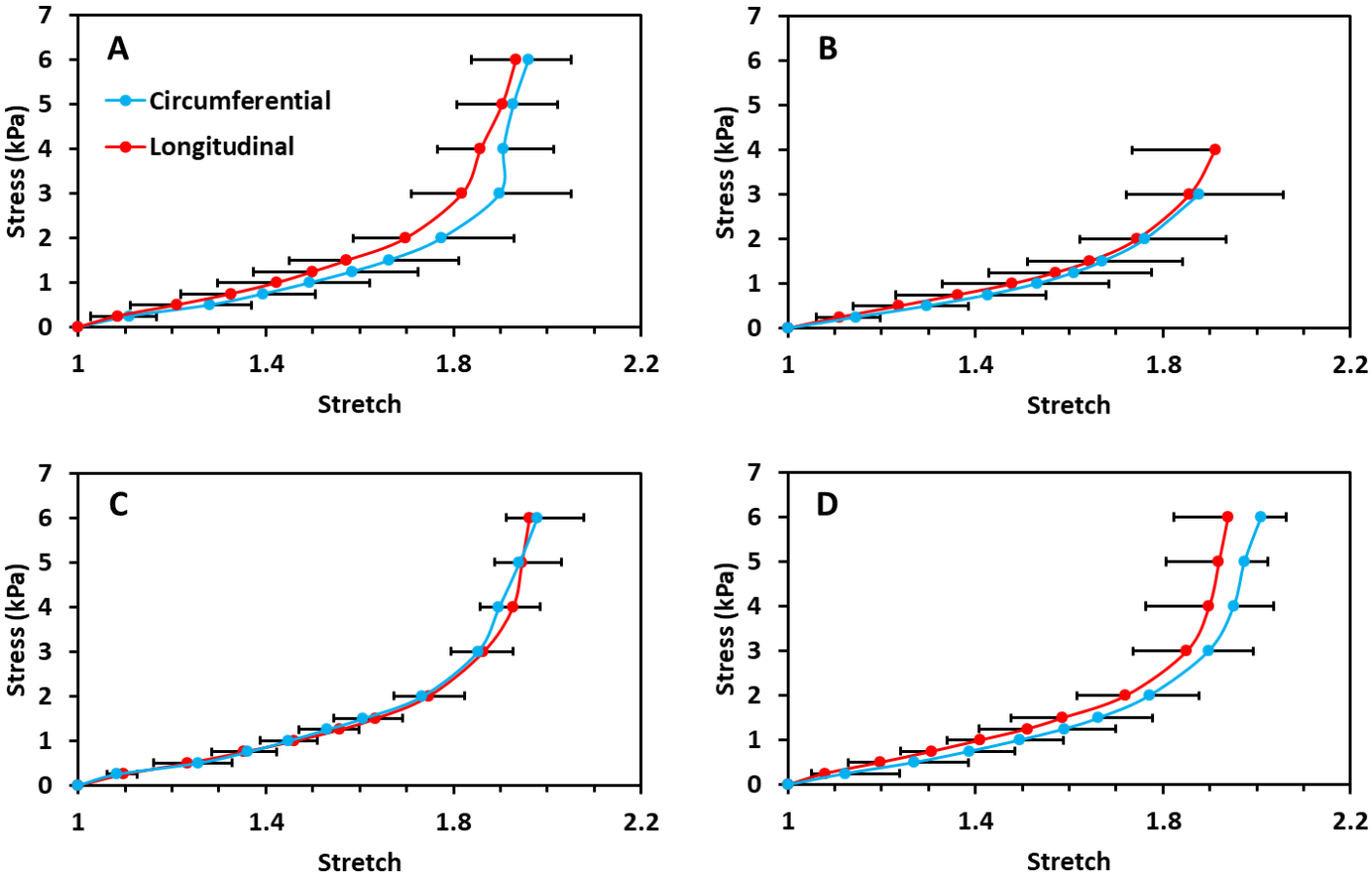

Figure S2: Average response of all regions to extension in the circumferential (blue) and longitudinal (red) directions. Regions are divided into **A)** bulbar proximal, **B)** bulbar distal, **C)** penile proximal, **D)** penile distal. No significant differences were observed between the two responses at any stress.

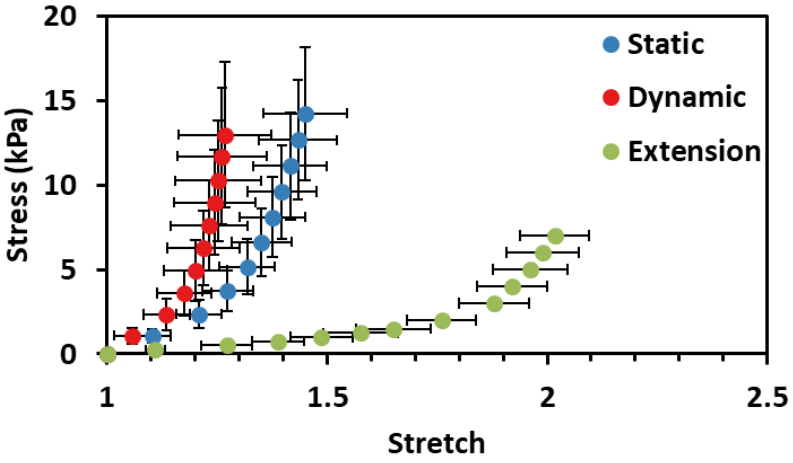

Figure S3: Comparison of the computed circumferential stress during intraluminal pressure application and circumferential extension testing.

Figure S3 shows a comparison of the circumferential stress calculated in the samples during the application of intraluminal pressure and the circumferential extension test results. There are obvious discrepancies between the two data sets, whereby the circumferential stress during intraluminal pressurisation at a given stretch is much higher than the corresponding stress during circumferential extension. A possible explanation for this is the ruffled lumen of the urethra which makes determining the actual wall thickness during intraluminal pressurisation impossible using the current data set. Furthermore, the eccentric lumen of the urethra means that an average wall thickness must be estimated. This is an issue because the urethras were incised caudally along the thinnest portion of the urethra prior to extension testing, meaning that the thickest portion of the urethra was subjected to circumferential extension, effectively reducing the stress in the system relative to the pressure diameter testing as the force is being distributed across a larger surface area.

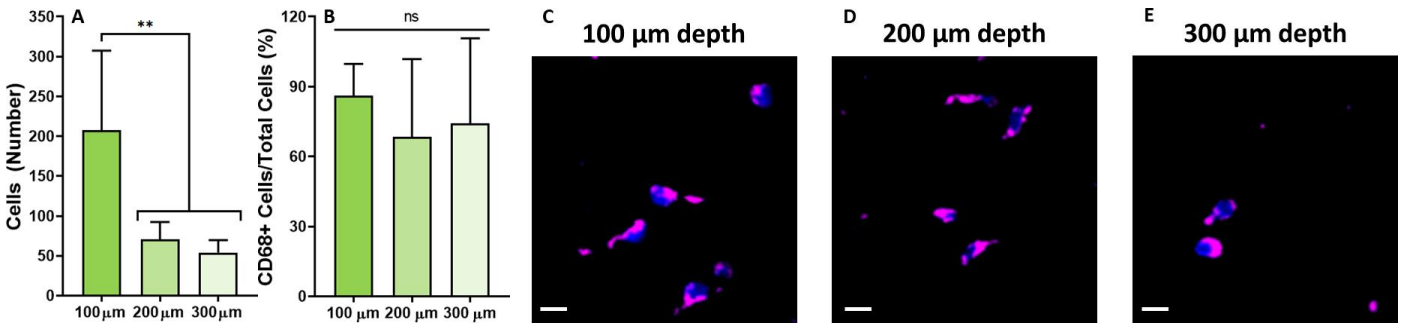

Figure S4: A-B) Analysis of cell number and ratio of CD68+ cells at different depths within the bilayered scaffold. **C-E)** Representative images of infiltrating cells at different depths.

Table S1: Pearson's correlation coefficients present between tissue composition and tissue mechanics as characterised by the application of static intraluminal pressure. r denotes the coefficient, * highlights p<0.05 and ** highlights p<0.01.

					Compliance (kPa^{-1})			Incremental Modulus (kPa)			
Variable		**Age**	**Stretch**	**Stiffness**	**Low**	**Mid**	**High**	**Overall**	**Low**	**Mid**	**High**
Elastin Content	r	-0.579	0.738	-0.142	0.751	0.298	0.205	-0.01	-0.501	-0.068	0.081
	p	0.102	0.023*	0.715	0.02*	0.437	0.596	0.98	0.17	0.863	0.837
Muscle Content	r	-0.583	0.85	-0.339	0.463	0.256	0.368	-0.3	-0.133	-0.218	-0.213
	p	0.1	0.004**	0.372	0.21	0.506	0.33	0.433	0.734	0.573	0.581
Collagen Content	r	-0.018	0.303	0.705	0.382	-0.597	-0.594	0.656	0.061	0.683	0.691
	p	0.964	0.428	0.034*	0.31	0.089	0.092	0.055	0.875	0.043*	0.039*

Table S2: Pearson's correlation coefficients present between overall urethral cross-section shape descriptors and tissue mechanics as characterised by the application of static intraluminal pressure. r denotes the coefficient, * highlights p<0.05 and ** highlights p<0.01.

					Compliance (kPa^{-1})			Incremental Modulus (kPa)				Composition
Variable		**Age**	**Stretch**	**Stiffness**	**Low**	**Mid**	**High**	**Overall**	**Low**	**Mid**	**High**	**Collagen**
Area	r	0.478	-0.578	-0.535	-0.24	0.487	0.576	-0.609	-0.315	-0.606	-0.643	-0.795
	p	0.194	0.103	0.137	0.534	0.183	0.105	0.082	0.409	0.084	0.062	0.01*
Perimeter	r	0.473	-0.597	-0.627	-0.354	0.551	0.59	-0.658	-0.205	-0.68	-0.701	-0.848
	p	0.199	0.09	0.071	0.35	0.124	0.095	0.054	0.597	0.044*	0.035*	0.004**
Max D	r	0.442	-0.573	-0.756	-0.491	0.627	0.68	-0.75	-0.033	-0.758	-0.799	-0.793
	p	0.234	0.107	0.018*	0.179	0.071	0.044*	0.02*	0.932	0.018*	0.01**	0.011*
Min D	r	0.513	-0.51	-0.421	-0.05	0.4	0.486	-0.531	-0.459	-0.529	-0.549	-0.696
	p	0.158	0.161	0.26	0.898	0.286	0.185	0.141	0.214	0.143	0.126	0.037*

Table S3: Pearson's correlation coefficients present between luminal cross-section shape descriptors and tissue mechanics as characterised by the application of static intraluminal pressure. r denotes the coefficient, * highlights p<0.05 and ** highlights p<0.01.

					Compliance (kPa^{-1})			Incremental Modulus (kPa)			
Variable		**Age**	**Stretch**	**Stiffness**	**Low**	**Mid**	**High**	**Overall**	**Low**	**Mid**	**High**
Area	r	0.384	-0.415	-0.474	-0.2	0.559	0.289	-0.229	-0.046	-0.43	-0.255
	p	0.307	0.266	0.197	0.605	0.118	0.451	0.553	0.907	0.249	0.508
Perimeter	r	0.067	0.148	-0.689	0.365	0.668	0.849	-0.751	-0.638	-0.693	-0.697
	p	0.863	0.703	0.04*	0.333	0.049*	0.004**	0.02*	0.065	0.038*	0.037*
Max D	r	0.35	-0.476	-0.193	-0.651	-0.018	0.014	-0.185	0.474	-0.177	-0.241
	p	0.356	0.196	0.618	0.058	0.964	0.971	0.634	0.198	0.648	0.533
Min D	r	0.413	-0.508	-0.373	-0.115	0.52	0.183	-0.213	-0.257	-0.43	-0.254
	p	0.27	0.162	0.323	0.767	0.151	0.637	0.581	0.504	0.248	0.509

Table S4: Overall and luminal dimensions of the human urethral samples characterised in this study.

	Overall Geometrical Features (mm)				Lumen Geometrical Features (mm)			
Sample	**Area**	**Perimeter**	**Max Diameter**	**Min Diameter**	**Area**	**Perimeter**	**Max Diameter**	**Min Diameter**
1	50.69	28.94	9.81	7.27	4.03	12.25	4.11	1.79
2	77.08	34.41	10.84	9.02	3.58	12.58	3.72	2.51
3	48.34	26.30	8.14	7.60	0.98	14.79	3.35	1.15
4	83.03	34.74	10.41	9.97	1.25	19.04	3.76	1.21
5	34.56	23.89	8.73	5.68	1.11	14.52	2.92	1.12
6	77.83	33.03	10.56	9.68	4.45	21.28	2.93	2.40
7	35.64	22.05	6.85	6.57	0.82	9.81	2.96	1.16
8	66.84	31.39	10.14	8.28	0.54	13.30	4.23	0.72
9	50.62	26.42	8.62	7.66	0.39	13.05	3.10	1.36
Average	58.29	29.02	9.34	7.97	1.91	14.51	3.45	1.49

Table S5: Modulus of human anterior urethral tissue in circumferential and longitudinal extension obtained from patient average response curves generated in this study. Studies that mechanically characterise SIS and UBM, the method of testing and the resulting modulus obtained from the high stretch region of the stress-strain curve.

Study	**Material**	**Method**	**Orientation**	**Modulus (MPa)**
Present Study	Human Anterior Urethral Tissue	Extension Testing	Circumferential	0.034±0.01
			Longitudinal	0.034±0.011
(Hiles et al., 1995)	Porcine SIS	Ring Tests	Circumferential	24±2.4
(Gilbert et al., 2008)	Porcine UBM scrapped circumferential and longitudinal	Equibiaxial Mechanical Test	UBMC Circumferential	6.9±1.1
			UBMC Longitudinal	17.6±4.8
			UBML Circumferential	25.9±10.6
			UBML Longitudinal	4.7±2
(Lu et al., 2005)	Cook porcine SIS	Equibiaxial Mechanical Test	Circumferential	21.49
			Longitudinal	33.35
(Raghavan et al., 2005)	Cook SIS and primary SIS	Uniaxial Extension (All Longitudinal)	Cook	26.26±14
			Primary Proximal	42±23
			Primary Distal	8.28±5
(Dahms et al., 1998)	Porcine UBM	Extension	Longitudinal	0.4±0.13
(Rosario et al., 2008)	Porcine UBM	Extension	Unspecified	1.53±0.21
(Brown et al., 2002)	Porcine UBM	Extension	Longitudinal	2±1
(Farhat et al., 2008)	Porcine UBM	Extension	Unspecified	0.65

Supplementary Information References

Brown, A. L. et al. (2002) '22 Week assessment of bladder acellular matrix as a bladder augmentation material in a porcine model', Biomaterials, 23(10), pp. 2179–2190. doi: 10.1016/S0142-9612(01)00350-7.

Dahms, S. E. et al. (1998) 'Composition and biomechanical properties of the bladder acellular matrix graft: Comparative analysis in rat, pig and human', British Journal of Urology, 82(3), pp. 411–419. doi: 10.1046/j.1464-410X.1998.00748.x.

Farhat, W. A. et al. (2008) 'Porcine bladder acellular matrix (ACM): protein expression, mechanical properties.', Biomedical materials (Bristol, England), 3(2), p. 25015. doi: 10.1088/1748-6041/3/2/025015.

Gilbert, T. W. et al. (2008) 'Collagen fiber alignment and biaxial mechanical behavior of porcine urinary bladder derived extracellular matrix', Biomaterials, 29(36), pp. 4775–4782. doi: 10.1016/j.biomaterials.2008.08.022.

Hiles, M. C. et al. (1995) 'Mechanical properties of xenogeneic small-intestinal submucosa when used as an aortic graft in the dog', Journal of Biomedical Materials Research, 29(7), pp. 883–891. doi: 10.1002/jbm.820290714.

Lu, S. H. et al. (2005) 'Biaxial mechanical properties of muscle-derived cell seeded small intestinal submucosa for bladder wall reconstitution', Biomaterials, 26(4), pp. 443–449. doi: 10.1016/j.biomaterials.2004.05.006.

Raghavan, D. et al. (2005) 'Physical characteristics of small intestinal submucosa scaffolds are location-dependent', Journal of Biomedical Materials Research - Part A, 73(1), pp. 90–96. doi: 10.1002/jbm.a.30268.

Rosario, D. J. et al. (2008) 'Decellularization and sterilization of porcine urinary bladder matrix for tissue engineering in the lower urinary tract', Regenerative Medicine, 3(2), pp. 145–156. doi: 10.2217/17460751.3.2.145.